Isotope Effect on Adsorbed Quantum Phases: Diffusion of H_{2} and D_{2} in Nanoporous Carbon

Cristian I. Contescu, Hongxin Zhang, Raina J. Olsen, Eugene Mamontov, James R. Morris, and Nidia C. Gallego

Phys. Rev. Lett. **110**, 236102 — Published 7 June 2013

DOI: 10.1103/PhysRevLett.110.236102

Isotope Effect on Adsorbed Quantum Phases: Diffusion of H_2 and D_2 in Nanoporous Carbon

Cristian I. Contescu[1],* Hongxin Zhang[1], Raina J. Olsen[1],
Eugene Mamontov[2], James R. Morris[1], and Nidia C. Gallego[1]
[1] *Materials Science and Technology Division, Oak Ridge National Laboratory, Oak Ridge, TN 37831, USA*
[2] *Neutron Scattering Sciences Division, Oak Ridge National Laboratory, Oak Ridge, TN 37831, USA*

Quasielastic neutron scattering of H_2 and D_2 in the same nanoporous carbon at 10-40 K demonstrates extreme quantum sieving, with D_2 diffusing up to 76 times faster. D_2 also shows liquid-like diffusion while H_2 exhibits Chudley-Elliott jump diffusion, evidence of their different relationships with the local lattice of adsorption sites due to quantum effects on intermolecular interactions. The onset of diffusion occurs at $22-25$ K for H_2 and $10-13$ K for D_2. At these temperatures, H_2 and D_2 have identical thermal de Broglie wavelengths that correlate with the dominant pore size.

It has been known that separation of deuterium from a H_2/D_2 mixture is possible through preferential adsorption [1] at low temperature on porous materials, but only recently it was understood that quantum effects [2] and restricted rotation [3] are what cause significant differences between adsorbed isotopes of the same chemical species, effects which can be utilized for their separation. Deuterium, with a higher mass than hydrogen, has a lower ground state energy, and thus may be more strongly adsorbed at low temperatures [4]. In nanoporous materials, when the thermal de Broglie wavelength λ_B is comparable with the effective confinement distance, quantization becomes important. This results in reduced dimensionality of the confined fluid and energy barriers for molecules entering the pores; in other words, the adsorbent acquires isotope separation properties [2]. Separation based on quantum effects has recently received intense scrutiny because of its potential for hydrogen isotope separation by preferential equilibrium adsorption of the heavier isotope [5–8]. Experimental studies have confirmed enhanced D_2 adsorption from H_2/D_2 mixtures on porous carbons [9], carbon nanotubes [10], zeolites [11], and metal organic frameworks [12] but the selectivity ratio was always lower than theoretical predictions [13].

Separation is also possible through kinetic quantum sieving. Bhatia et al. [14–17] predicted that, at sufficiently low temperatures, hydrogen diffuses slower than deuterium when confined in nanopores with size close to the molecular diameter. For diatomic molecules, quantized rotation [3, 18] and roto-translation coupling [19] introduce strong orientation effects which increase the energy barriers for self-diffusion, and dramatically favor transport of D_2 over H_2 [17]. Bhatia et al. used quasielastic neutron scattering (QENS) and experimentally confirmed differences in diffusivity between H_2 and D_2 in zeolite and carbon molecular sieves (CMS) at low temperatures [20–22]. The kinetic selectivity (ratio of the D_2 self-diffusion coefficient to that of H_2) had inverse quadratic temperature variation, with a maximum of about 2 for Takeda 3A CMS at the lowest temperature investigated (40 K). The T^{-2} variation of kinetic selectivity (as opposed to the T^{-1} variation in classical systems) is a signature of the diffusion of the lighter isotope being more hindered by quantum effects [22]. These experiments were conducted at temperatures above the critical point of bulk H_2 (33.2 K) and D_2 (38.3 K). At lower temperatures, when molecules may form a liquid or solid phase on the adsorbent, intermolecular interactions will likely result in further differences between the isotopes. Since quantum effects vary inversely with temperature, low temperature measurements should demonstrate even higher values of kinetic selectivity.

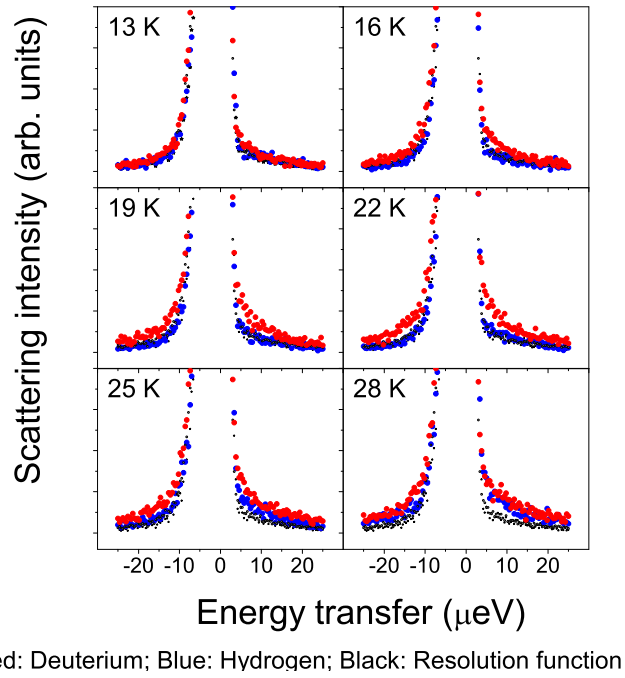

FIG. 1. (Color online.) Raw scattering intensity data showing the scattering in vacuum and at several temperatures after loading H_2 or D_2 . Data for H_2 were collected in a previous experiment [23].

We previously reported [23] QENS results for H_2 confined in narrow nanopores (< 7 Å) of polyfurfuryl alcohol-derived activated carbon (PFAC) at tempera-

tures (10-37 K) crossing the triple point (13.9 K) and critical point of bulk H_2. Here we report new QENS results for D_2 adsorbed on the same carbon (Fig. 1), obtained using the same equipment, procedure, and conditions. At temperatures lower than those explored by previous researchers, we find significantly higher D_2/H_2 kinetic selectivity than previously reported [22]. In addition, the two isotopes, exhibit completely different diffusion mechanisms due entirely to quantum effects (Fig. 2).

PFAC was obtained and characterized as previously reported [23, 24]. Briefly, it has 1530 m^2/g BET surface area [25] and 0.99 cm^3/g total pore volume, of which 0.21 cm^3/g is contained in narrow nanopores (H_{eff} <7 Å). Here H_{eff} is the effective pore width between solid carbon walls, defined as $H_{eff} = H$-3.4 Å, where 3.4 Å is the carbon atom diameter and H is the center-to-center distance between carbon atoms in opposite pore walls [26].

QENS measurements were performed on the backscattering spectrometer (BASIS) of the Spallation Neutron Source at Oak Ridge National Laboratory [27]. Following our previous procedure [23], about 1g of PFAC sample was outgassed at 400°C to $< 10^{-4}$ Pa and sealed under dry He in the aluminum cell used for measurements. The instrumental resolution function, determined from the background spectrum at 7 K for PFAC under vacuum, has a half width at half maximum (HWHM) of 1.5 μeV. High purity D_2 was adsorbed to saturation at 77 K. The excess gas was evacuated ($< 10^{-4}$ Pa) at 35 K, the cell was sealed, and temperature was lowered to 10 K. QENS spectra were collected every 3 K from 10 to 40 K, with 1.5-2 h acquisition times at each temperature. As temperature increased, the quasielastic (QE) scattering signal broadened continuously due to the gradually increasing mobility of adsorbed molecules. Using DAVE software [28] the QE scattering at each temperature was obtained from the fit of scattering intensity vs. energy transfer. The fit included elastic (delta function) and QE (Lorentz function with HWHM dependent on momentum transfer, Q) components, broadened by the instrumental resolution, plus a linear background.

Figure 1 shows raw QENS data for the two isotopes measured at several temperatures. Two identical background plots measured separately before introduction of D_2 (or H_2) are also shown. When the adsorbed gas is present, the increase of temperature produces gradual broadening of the scattering signal profile which departs from the elastic line recorded in vacuum. The broadening of the scattering line begins at lower temperatures in the D_2-loaded carbon than in the H_2-loaded sample.

This broadening is quantified in Figure 2, which shows the HWHM at each Q. Results indicate that D_2 becomes mobile between 10 and 13 K; in contrast, H_2 became mobile on PFAC between 22 and 25 K [23]. Below these temperatures, scattering is barely distinguishable

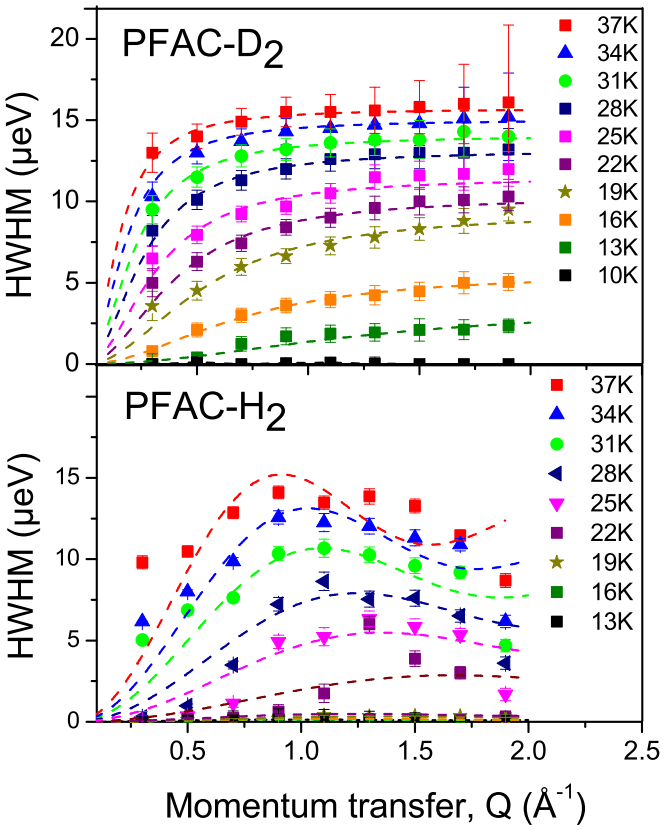

FIG. 2. (Color online.) Q-dependence of HWHM of the scattering component for D_2 and H_2 in PFAC. Dotted lines show model fitting according to Eq. 1 for D_2 and Eq. 2 for H_2.

from the instrument resolution. Since all conditions were identical, including the amount of H_2 (D_2) adsorbed (∼ 35 % of monolayer coverage based on the BET surface area), the results can be accurately compared. The main differences are that (1) diffusion of H_2 is more restricted than D_2, based on the mobility onset temperatures; and (2) the two isomers have different diffusion mechanisms, as shown by the variation of HWHM of the QE component versus Q (Fig. 2, where H_2 data are re-plotted from Ref. [23]). The D_2 data were fitted well by a liquid-like diffusion model [29] where particles execute random jumps of lengths a distributed as $a(L) = Le^{-L/L_o}$, whose signature is a sigmoidal HWHM variation with Q:

$$HWHM(Q) = \frac{\hbar}{\tau}(1 - \frac{1}{1 + Q^2 < L^2 > /6}); D = \frac{< L^2 >}{6\tau}. \quad (1)$$

In contrast, the non-monotonic behavior of the H_2 data cannot be fit using Eq. 1. Instead, this data was fit by the fixed-length jump model ($L = Lo$ = const) initially developed by Chudley and Elliott (CE) to describe a liquid phase close to its melting point which locally has a lattice-like structure [30]

$$HWHM(Q) = \frac{\hbar}{\tau}(1 - \frac{1}{QL_o} sin(QL_0)); D = \frac{L_o^2}{6\tau}. \quad (2)$$

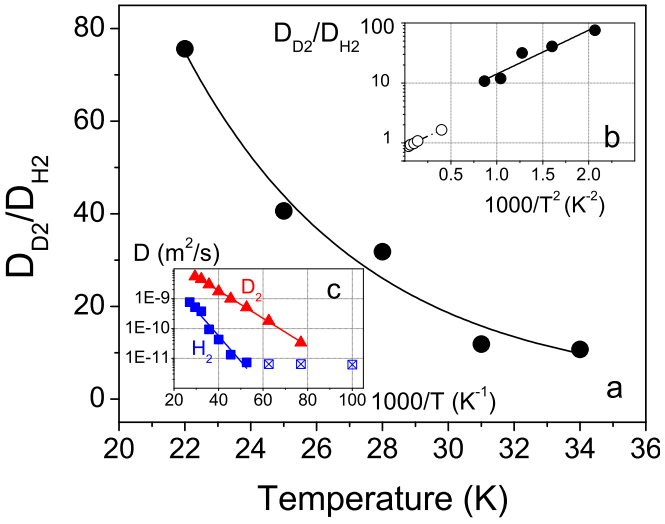

FIG. 3. (Color online.) (a) Temperature dependence of kinetic selectivity. (b) Kinetic selectivity variation versus T^{-2} showing quantum molecular sieving of quantized molecules (• this work; ◦ data from Ref. [22]); (c) Classical plot of diffusion coefficients showing delayed mobility onset for adsorbed H_2.

This model describes dynamic behavior when motions near a particular site are occasionally interrupted by discrete jumps to neighboring vacant lattice sites at a well-defined distance. The model has been generalized to jump diffusion on 2D or 3D lattice. The CE jump diffusion model was also found to fit data well for H_2 in a different porous carbon in our previous QENS study [23].

Diffusion coefficients were calculated from fit parameters L and τ (residence time). The kinetic selectivity is shown in Figure 3(a), and varies between 10 and 76. To our best knowledge, these are the highest kinetic selectivity values ever measured for D_2/H_2 quantum sieving on carbons. On a logarithmic scale, selectivity depends linearly on T^{-2}, as expected for self-diffusion of quantized H_2 and D_2 [22]. Figure 3(b) compares our data with those measured at higher temperatures for Takeda 3A CMS [22]. Classical analysis of diffusion coefficients, $ln(D) = ln(D_o) - E_{act}/(k_BT)$, in Fig. 3(c) gives E_{act}/k_B =110 K,$D_o = 1.58 \times 10^{-7}$ m^2/s for D_2; and E_{act}/k_B = 229 K, $D_o = 4.31 \times 10^{-7}$ m^2/s for H_2. Diffusion of quantized molecules at low temperature is further analyzed in the supplementary information.

The difference in the HWHM variation versus momentum transfer (Fig. 2) suggests that the isotopes diffuse quite differently. Since the carbon substrate and the experimental conditions were the same, the explanation for this difference must be due to the different quantum nature of the isotopes at low temperature. Phase diagrams for each hydrogen isotope on graphite derived from specific heat data [31] show a solid triangular $\sqrt{3}\times\sqrt{3}$ phase in register with the underlying graphene lattice at coverages below 65 % of a monolayer, which melts into a 2D fluid phase at temperatures between 10-18 K for D_2 and 10-21 K for H_2, depending on coverage. Wiechert [31] hypothesized that the formation and stability of the registered phase, which is quite different than the bulk solids, is due to the repulsive intermolecular interactions between the molecules. The zero-point motion of the molecules adds a repulsive contribution to the intermolecular interactions, and tends to localize the particles into the potential minima of the graphite surface. The larger zero-point motion of H_2 as compared to D_2 results in a slightly higher melting temperature of the solid registered triangular lattice at high coverage.

Previous models of quantum sieving have ignored intermolecular interactions; but below the critical point they can not be ignored. Because of stronger quantum effects, the effective size is larger for H_2 than for D_2, resulting in more repulsive effective H_2-H_2 interactions than for D_2. Due to its smaller zero-point motion, D_2 prefers a more closely packed structure than H_2 and its registered triangular lattice is less stable. Our preliminary calculations support this model [32]. Thus when adsorbed on graphite, we expect D_2 to be closer to a 2D liquid phase after becoming mobile, while H_2 still interacts locally with a lattice-like structure. This picture is supported by low temperature neutron scattering measurements of H_2 and D_2 adsorbed on Grafoil [33, 34], which also found differences in the behavior of the isotopes above their melting temperatures. Nielsen et al. [33] concluded that on melting, D_2, 'is probably gas-like,' while H_2 'molecules show solid like behavior up to 31 K' [34].

To explain the difference between the diffusion mechanism of the two isotopes observed here, we argue that a similar model applies locally in porous carbons. Detailed STEM images obtained recently for PFAC [35] show convincingly that this material is comprised of curved graphene sheets with sizes of a few nanometers. Examination of over a hundred atomic resolution STEM images show that the basic building blocks of PFAC are composed mostly of carbon atoms arranged hexagonally as in graphene, interrupted occasionally by 5- and 7-atom rings which induce local curvature (as in Figs. 3 c,d of Ref. [35]). Our 3D model of graphitic sheets in nanoporous carbons developed from those images (Fig. 6 of Ref. [35]) is that dislocation lines of nonhexagonal defects define large areas of 2D ordered graphene extending up to 2 or 3 nm. However, the spatial range accessed in our QENS experiments is shorter, only about 20 Å, calculated as $d = 2\pi/Q$ where $Q = 0.3$ Å^{-1} is the lowest Q value. On these almost flat or weakly undulated graphenes, the sub-monolayers of adsorbed H_2 (D_2) are expected to experience short range arrays of local potential minima not much different than on exfoliated graphite. Adsorbed H_2 would be constrained to a similar triangular array of adsorption sites which would allow only constant jump lengths between occupied and free positions, while preventing closer H_2-H_2 approach

due to strong repulsions.

This picture is strongly supported by the good match between the nearest-neighbor distance in the triangular lattice of adsorption sites (4.26 Å) on graphite [33] with the jump length fit parameters for our QENS data for H_2 on PFAC (4.02 ± 0.82 Å) and UMC (4.74 ± 0.67 Å). These jump lengths do not change much with temperature. On the other hand, after becoming mobile, D_2 exhibits jumps lengths that increase with temperature (from 3.6 Å at 16 K to 16.2 Å at 37 K).

In addition to the difference in the shape of the QE scattering patterns, a large difference exists between the temperatures where mobility is first observed: 22-25 K for H_2 and 10-13 K for D_2. However, on another ultramicroporous porous carbon (UMC) H_2 becomes mobile at a slightly lower temperature (19-22 K), while its diffusion obeys the same Chudley-Elliott mechanism [23]. While the consistency of the CE mechanism for H_2 on different carbons supports our hypothesis of a strongly correlated adsorbed H_2 layer in register with the graphene-like lattice, the variation in the mobility onset temperature for the two isotopes on the same carbon points to another quantum effect. Narrow porosity restricts the mobility of quantized molecules. We calculated the pore size distribution (PSD) from CO_2 adsorption data collected at 273 K using the non-local density functional theory (NLDFT) and the slit-shaped pore model (Quantachrome software). In this model [36], porous carbon is regarded as a collection of independent pores of various widths. At very low temperature, adsorbates populate first the pores with highest adsorption energy. From the cumulative pore surface distribution versus pore width (Fig. 4) we estimate that H_2 (D_2) with average surface densities of about 35 % of a BET monolayer is located with high probability in the nanopores with 3.5 Å< H_{eff} <5.5 Å. The local adsorbate density in these preferentially occupied pores is much higher than the mean surface coverage based on BET surface area, as theoretically predicted [37] and confirmed experimentally [38]. At room temperatures, these narrow nanopores can accommodate one or two monolayers of adsorbed H_2 or D_2. However, at very low temperatures, the higher zero-point motion energy in narrow nanopores will create a preference for larger pores, particularly for lighter H_2.

We hypothesize that, on raising the temperature, molecules become mobile when the effective size of the quantized species becomes smaller than a characteristic size parameter of the adsorbent. The hard-core size of quantized molecules was defined [21] as the C−H_2 separation σ_0 where the quartic Feynman-Hibbs (FH) repulsive potential is $U_{FH}(\sigma_0)$ =0 (see supplementary material). The thermal de Broglie wavelength $\lambda_B = h/\sqrt{(2\pi\mu k_B T)}$is a measure of position delocalization. The sum $\lambda_B + \sigma_0 = \rho$ defines the smallest pore width that allows detectable mobility at the time scale of our measurements based on momentum transfer with impinging neutrons. Thus defined, ρ is similar with the quantum effective pore size introduced by Liu et al. [39] for quantum sieving on metal-organic frameworks. Figure 4(a) shows the variation of λ_B and ρ with temperature. Comparison with Fig. 4(b) suggests that the mobility occurs at temperatures where ρ becomes comparable with the prevailing effective pore width (∼5.6 Å) in PFAC. H_2 becomes mobile at a higher temperature than D_2 because of its larger quantum spreading. For additional confirmation we plot in Figure 4(c) the PSD of UMC [40]. The lower mobility onset temperature for UMC correlates with UMC having a slightly larger statistical mode of nanopores width (∼6 Å). In line with Kumar and Bhatia [14] it appears that steric hindrance caused by quantum delocalization (λ_B) and enlarged effective size of quantized molecules (σ_0) are important enabling factors of D_2/H_2 separation at these low temperatures. The difference between PFAC and UMC porosity is expected to significantly change their respective D_2/H_2 selectivity at higher temperatures (see supplementary information).

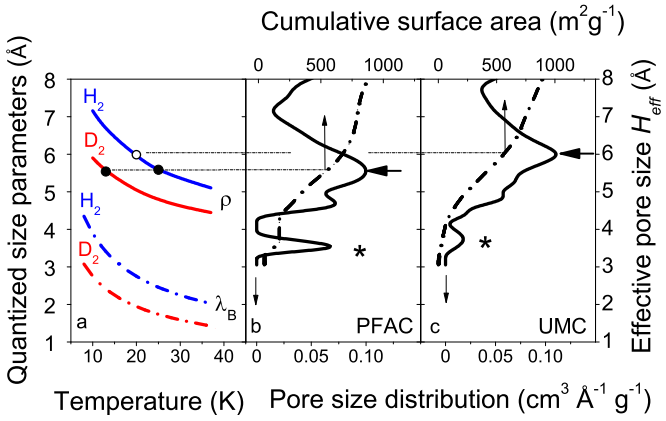

FIG. 4. (Color online.) (a) Temperature variation of de Broglie wavelength (λ_B) and size parameter (ρ) for quantized molecules. Marks show mobility onset temperatures for H_2 and D_2 on PFAC (this work, • and for H_2 on UMC ∘, Ref. [23]). (b) Differential PSD and cumulative surface area distribution versus pore size for PFAC and (c) UMC.

In conclusion, high kinetic selectivity for D_2/H_2 quantum sieving was found for PFAC at temperatures between the triple point and the critical point of bulk gases, where D_2 is more mobile than H_2. In a temperature window of about 10 K the two isotopes exhibit distinct diffusion mechanisms which we explain by different registry of the two isotopes relative to the lattice of adsorption sites caused by the different strength of quantum effects on their intermolecular interactions. We also observed that the thermal de Broglie wavelength of H_2 and D_2 at their respective mobility onset temperatures are identical and correlated with the dominant pore size.

ACKNOWLEDGMENTS

This work was supported by the Materials Science and Engineering Division, Office of Basic Energy Sciences, U.S. Department of Energy. QENS experiments were conducted at Oak Ridge National Laboratory's Spallation Neutrons Source supported by the Scientific User Facility Division, Office of Basic Energy Sciences, U.S. Department of Energy. HZ acknowledges appointment under the ORNL Postdoctoral Associate Program administered jointly by Oak Ridge Institute for Science and Education and Oak Ridge Associated University. RJO performed quantum calculations with support from the U.S. Department of Energy Office of Energy Efficiency and Renewable Energy (DOE-EERE) postdoctoral research award under the EERE Fuel Cell Technologies Program.

* contescuci@ornl.gov

[1] D. White and W. J. Haubach, J. Chem. Phys. **30**, 1368 (1959).
[2] J. J. M. Beenakker, V. D. Morman, and S. Y. Krylov, Chem. Phys. Lett. **232**, 379 (1995).
[3] B. C. Hathorn, B. G. Sumpter, and D. W. Noid, Phys. Rev. A **64**, 022903 (2001).
[4] A. Katorski and D. White, J. Chem. Phys. **40**, 3183 (1964).
[5] Q. Y. Wang *et al.*, Phys. Rev. Lett. **82**, 956 (1999).
[6] P. Kowalczyk *et al.*, Langmuir **23**, 3666 (2007).
[7] P. Kowalczyk *et al.*, J. Phys. Condens. Matter. **21**, 144210 (2009).
[8] A. Gotzias and Th. Steriotis, Molec. Phys. **110**, 1179 (2012).
[9] X. Zhao *et al.*, J. Phys. Chem. B. **110**, 9947 (2006).
[10] H. Tanaka *et al.*, J. Am. Chem. Soc. **127**, 7511 (2005).
[11] X.-Z. Chu *et al.*, J. Phys. Chem. B. **110**, 22596 (2006).
[12] B. Chen *et al.*, J. Am. Chem. Soc. **130**, 6411 (2008).
[13] J. Cai, Y. Xing, and X. Zhao, RSC Advances **2**, 8579 (2012).
[14] A. V. Anil Kumar and S. K. Bhatia, Phys. Rev. Lett. **95**, 245901 (2005); **96**, 119901(E) (2006).
[15] A. V. Anil Kumar and S. K. Bhatia, J. Phys. Chem. C **112**, 11421 (2008)).
[16] Y. Wang and S. K. Bhatia, J. Phys. Chem. C **113**, 14953 (2009).
[17] M. Hankel *et al.*, Phys. Chem. Chem. Phys. **13**, 7834 (2011).
[18] G. Garberoglio, Eur. Phys. J. D **51**, 185 (2009).
[19] G. Garberoglio and J. K. Johnson, ACS NANO **4**, 1703 (2010).
[20] A. V. Anil Kumar, H. Jobic, and S. K. Bhatia, J. Phys. Chem. B **110**, 16666 (2006).
[21] A. V. Anil Kumar, H. Jobic, and S. K. Bhatia, Adsorption **13**, 201 (2007).
[22] T. X. Nguyen, H. Jobic, and S. K. Bhatia, Phys. Rev. Lett. **105**, 085901 (2010).
[23] C. I. Contescu *et al.*, Carbon **50**, 1071 (2012).
[24] H. Zhang *et al.*, Carbon **50**, 5278 (2012).
[25] S. Brunauer, P. H. Emmett, and E. Teller, J Am. Chem. Soc. **60**, 309 (1938).
[26] J. Jagiello, A. Anson, and M. T. Martinez, J Phys. Chem. **8**, 4531 (2006).
[27] E. Mamontov and K. W. Herwig, Rev. Sci Instr. **82**, 085109 (2011).
[28] R. T. Azuah *et al.*, Res. Natl. Inst. Stan. Technol. **114**, 341 (2009).
[29] P. A. Egelstaff, *An Introduction to the Liquid State* Oxford University Press, New York, (1992) pp. 46–48.
[30] C. T. Chudley and R. J. Elliot, Proc. Phys. Soc. London **77**, 353 (1961).
[31] H. Wiechert, Physica B **169**, 144 (1991).
[32] R. J. Olsen, unpublished.
[33] M. Nielsen, J. P. McTague, and W. Ellenson, J. Phys. (Paris) **38**, 10 (1977).
[34] M. Nielsen and W. Ellenson, in *Proc. 14th Intl. Conf. Low Temperature Physics, 1975* edited by Ed. M Krusius and M Vuorio (North Holland, Amsterdam), pp. 437–440.
[35] J. Guo *et al.*, Small **8**, 3283 (2012).
[36] P. I. Ravikovitch *et al.*, Langmuir **16**, 2311 (2000).
[37] L. Peng and J. R. Morris, J. Phys. Chem. C **114**, 15522 (2010).
[38] N. C. Gallego *et al.*, J. Am. Chem. Soc. **133**, 13794 (2011).
[39] D. Liu *et al.*, Ind. Eng. Chem. **51**, 434 (2012).
[40] V. V. Bhat *et al.*, Carbon **48**, 1331 (2010).